

# Molecular-Dynamics Simulation of a Glassy Polymer Melt: Incoherent Scattering Function

C. Bennemann, J. Baschnagel\*, and W. Paul

*Institut für Physik, Johannes-Gutenberg Universität,  
Staudinger Weg 7, D-55099 Mainz, Germany*

## Abstract

We present simulation results for a model polymer melt, consisting of short, nonentangled chains, in the supercooled state. The analysis focuses on the monomer dynamics, which is monitored by the incoherent intermediate scattering function. The scattering function is recorded over six decades in time and for many different wave-vectors which range from the size of a chain to about three times the maximum position of the static structure factor. The lowest temperatures studied are slightly above  $T_c$ , the critical temperature of mode-coupling theory (MCT), where  $T_c$  was determined from a quantitative analysis of the  $\beta$ - and  $\alpha$ -relaxations. We find evidence for the space-time factorization theorem in the  $\beta$ -relaxation regime, and for the time-temperature superposition principle in the  $\alpha$ -regime, if the temperature is not too close to  $T_c$ . The wave-vector ( $q$ -) dependence of the nonergodicity parameter, of the critical amplitude, and the  $\alpha$ -relaxation time are in qualitative agreement with calculations for hard spheres. For  $q$  larger than the maximum of the structure factor the  $\alpha$ -relaxation time  $\tau_q$  already agrees fairly well with the asymptotic MCT-prediction  $\tau_q \sim q^{-1/b}$ . The behavior of the relaxation time at small  $q$  can be rationalized by the validity of the Gaussian approximation and the value of the Kohlrausch stretching exponent, as suggested in neutron-scattering experiments.

PACS: 61.20.Ja, 64.70.Pf, 61.25.Hq, 83.10.Nn

submitted to *Phys. Rev. E* on August 19, 2018

## I. INTRODUCTION

During the past decade, numerous experiments and simulations have focused attention on the dynamics of supercooled liquids in a temperature region about fifty degrees above the calorimetric glass transition [1,2,3,4,5]. This interest has been elicited by the development of the so-called mode-coupling theory (MCT) [5,6,7]. Mode-coupling theory predicts that there is a critical temperature  $T_c$  above  $T_g$ , where the dynamics of the glass former qualitatively changes from a liquid-like to a solid-like behavior. The onset of this change is manifested by a two-step decay of dynamic correlation functions, which couple to density fluctuations.

---

\*To whom correspondence should be addressed. Email: baschnag@flory.physik.uni-mainz.de

These correlation functions can be measured in experiments and computer simulations. The distinguishing feature of the theory is that it makes universal, system-independent predictions about the shape of the time correlation functions, that there are constraining relationships between various theoretical quantities, and that key, nonuniversal parameters can be expressed in terms of the glass former's static structure.

Especially the latter point opens the possibility of a direct comparison between theory and experiment or simulation. Such comparisons are, however, predicated upon having accurate data for the temperature dependence of the static structure factor at hand. Therefore, they have only been performed for few, simple systems, such as hard-sphere-like colloidal particles [8] or computer models of soft spheres [9], and binary Lennard-Jones mixtures [10].

On the other hand, most tests of MCT have concentrated on the universal predictions by adjusting the system-specific parameters. This fit procedure must simultaneously optimize at least three free parameters. It is rather involved and further complicated by the fact that the theoretical predictions are only valid asymptotically in a narrow temperature interval around  $T_c$ , and that the microscopic (vibrational) time scales have to be well separated from those of the structural relaxation. These drawbacks have led to a criticism of the significance of the experimental evidence for the theory [11], but also to extensions of MCT to tackle problems, like the interference of vibrational and relaxational time scales [12], orientational degrees of freedom [13], and corrections to the asymptotic behavior [14,15]. This situation suggests that further tests may be beneficial.

In the present paper we want to discuss the results of a molecular-dynamics (MD) simulation for a polymer melt and the analysis of the incoherent intermediate scattering function by the idealized mode-coupling theory. Comparable applications of the theory to polymer melts have already been performed in experiments and simulations. One of the earliest applications were neutron scattering experiments of polybutadiene [16]. These experiments found the predicted square-root behavior for the temperature dependence of the nonergodicity parameter below  $T_c$ , suggested an in-phase variation of the coherent  $\alpha$ -relaxation time with the static structure factor, and provided evidence for time-temperature superposition above  $T_c$ . These studies mainly focused on the  $\alpha$ -relaxation. A detailed line shape analysis in the  $\beta$ -relaxation regime was not made. Such an analysis was attempted in dielectric relaxation experiments of poly(ethylene terephthalate) [17]. The experiments are complicated by the fact that poly(ethylene terephthalate) has a high tendency to crystallize, and that a  $\beta$ -peak masks the MCT  $\beta$ -process. Nevertheless, the experiments confirmed some of the idealized predictions, but also claimed that there are severe deviations, especially below  $T_c$ . Close to and below  $T_c$  deviations are expected due to ergodicity restoring processes. Usually, the extended MCT [18] is then applied to account for these processes. However, a recent reanalysis [19] of the dielectric data indicates that the deviations cannot be explained in this way. Instead, a higher order scenario, an  $A_3$ -singularity, has to be used. In applications to other structural glass formers these higher-order singularities are less common, but some studies suggest that they could be pertinent to partially crystalline polymers [20,21].

On the simulation side, the glassy behavior of polymer melts has been studied by Monte-Carlo simulations of the bond-fluctuation lattice model [22,23,24]. These simulations deal with short, nonentangled chains, and have been restricted to temperatures above  $T_c$ . A comparison with MCT indicated that a quantitative description of the  $\beta$ -relaxation is possible if the extended theory is used [25]. Despite this agreement, there are still some points which

could be improved upon. On the one hand, the simulations were performed at constant volume, whereas experiments are usually done at constant pressure, and the underlying lattice structure precludes all phonon contributions to the short-time dynamics. On the other hand, the simulation data were not completely equilibrated. They still exhibited very slow physical aging processes. These aging processes effectively correspond to additional relaxation channels which are not contained in the idealized MCT. Although it is interesting that the extended MCT is able to describe such a situation – especially when taking into account the current intensive research on physical aging below  $T_c$  [26,27] –, the simulations do not meet the theoretical premise of thermal equilibrium.

Both drawbacks are removed by the present MD-simulation. It is done at constant pressure and equilibrated on all length scales which we will discuss, i.e., at low temperatures the simulation time spent for equilibration exceeded by one order of magnitude the time, over which actual dynamical measurements were performed after equilibration. Some details of the model, of its static properties, and of the simulation are compiled in the next section. The subsequent section is split into two parts. The first describes the analysis of the  $\beta$ -relaxation, and the second that of the  $\alpha$ -relaxation. The last section summarizes the main results.

## II. MODEL, STATIC RESULTS, AND SIMULATION TECHNIQUE

This section briefly reviews some characteristics of the model. A detailed description of its properties and of the simulation technique can be found in Ref. [28].

The simulations were done with linear, nonentangled, monodisperse chains of length  $N = 10$ . All monomers interact by a truncated and shifted Lennard-Jones (LJ) potential,  $U_{\text{LJ}}(r) = 4\epsilon[(\sigma/r)^{12} - (\sigma/r)^6] + C$ . The constant  $C = 0.00775$  assures that the potential vanishes if  $r \geq 2r_{\text{min}} = 2 \times 2^{1/6}\sigma$ , where  $r_{\text{min}}$  is the minimum position. Temperature and distances are measured in units of  $\epsilon/k_B$  and  $\sigma$ , respectively, and time is measured in units of  $(m\sigma^2/\epsilon)^{1/2}$ , where the mass is set to unity.

In addition, there is a FENE-potential between bonded monomers along the backbone of a chain, i.e.,  $U_{\text{F}}(r) = -15R_0^2 \ln[1 - (r/R_0)^2]$  with  $R_0 = 1.5$ . With these parameters the superposition of the FENE- and LJ-potentials generates a steep effective bond-potential with a minimum at about  $0.96\sigma$

In our study a melt configuration contained 120 polymers, and ten configurations were simulated at each temperature to improve the statistics. The simulation procedure consisted of two steps. First, the volume was allowed to fluctuate in a simulation at a given temperature and pressure (always  $p = 1$  – the influence of pressure is studied in Ref. [29]) to determine the equilibrium density at this thermodynamic state point. Fixing then the resulting volume the subsequent runs used the Nosé-Hoover thermostat to simulate in the canonical ensemble. All dynamic properties calculated are results from these canonical simulations. In order to equilibrate the system, each chain was propagated several times over the distance of radius of gyration before starting the analysis. This time suffices so that the incoherent scattering functions have decayed to zero for all wave-vectors (except for  $q < 2$  at  $T = 0.46$ ).

The particular choice of the bonded and nonbonded potentials has two main consequences for the static properties of the model. First, the chains do not become stiffer with decreasing

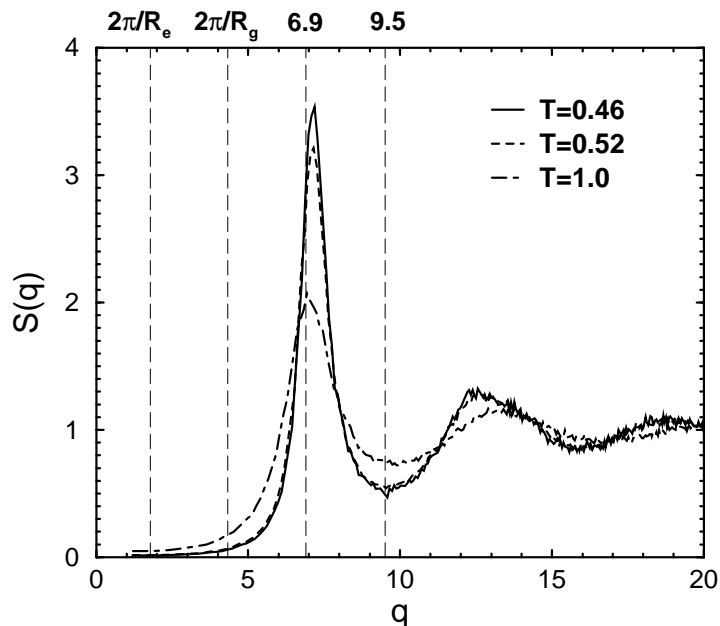


FIG. 1. Temperature dependence of the melt's structure factor. The temperatures span the interval from the normal liquid ( $T = 1$ ) to the supercooled state ( $T = 0.46$ ) of the melt. The lowest temperature is slightly above  $T_c \simeq 0.45$ . In the mode-coupling analysis mostly  $q = 3, 6.9, 9.5$  are used. The smallest  $q$ -value probes the size of a chain (end-to-end distance:  $R_e \simeq 12.3$ , radius of gyration:  $R_g \simeq 2.09$ ), whereas the larger wave-vectors correspond to intermonomer distances.

temperature. In the interesting temperature region ( $T < 0.7$ ) the end-to-end distance,  $R_e$ , and the radius of gyration,  $R_g$ , are essentially constant:  $R_e^2 = 12.3 \pm 0.1$ ,  $R_g^2 = 2.09 \pm 0.01$ . Second, the monomer distance 0.96, favored by the bond-potential, is incompatible with multiples of  $r_{\min}$ , and thus with crystalline ordering. This is illustrated by the static structure factor of the melt in Fig. 1<sup>1</sup>. At small wave-vectors, the structure factor is of the order of 0.01, indicating that the melt has a low compressibility, then it raises and exhibits an amorphous halo close to  $q = 6.9$ , corresponding to the nearest-neighbor packing of the monomers, and finally decreases again and begins oscillating to gradually approach 1 for large  $q$ . This structure is characteristic of the liquid state and present at all temperatures. With decreasing temperature the maxima and minima become sharper, and the position of the first maximum slightly shifts to larger  $q$ -values because the density of the melt increases.

---

<sup>1</sup>This figure extends the data of Fig. 6 in Ref. [28]. Note that we chose the conventional normalization in the present case contrary to Ref. [28]. In Fig. 1,  $S(q)$  tends to the isothermal compressibility divided by that of the ideal gas, i.e., to  $\rho T \kappa_T$ , if  $q \rightarrow 0$ , whereas it approaches  $(\rho T \kappa_T / \text{total number of monomers})$  in Ref. [28].

### III. IDEALIZED MODE-COUPLING ANALYSIS

Close to the critical temperature mode-coupling theory predicts a two-step relaxation behavior for dynamic correlation functions that couple to density fluctuations, like the incoherent intermediate scattering function,

$$\phi_q^s(t) = \frac{1}{M} \sum_{m=1}^M \left\langle \exp(\mathbf{i}q \cdot [\mathbf{r}_m(t) - \mathbf{r}_m(0)]) \right\rangle, \quad (1)$$

where  $M$  stands for the total number of monomers in the melt. The expected two-step relaxation gradually develops for  $T \leq 0.55$  in our model. Therefore the following analysis focuses on this temperature region. It is divided into two parts. First, we discuss the  $\beta$ -relaxation regime, and then the final structural decay, the  $\alpha$ -relaxation.

#### A. $\beta$ -relaxation regime

The  $\beta$ -relaxation regime is defined as the time window, where the correlator  $\phi_q^s(t)$  is close to the nonergodicity parameter  $f_q^{\text{sc}}$ , i.e.,  $|\phi_q^s(t) - f_q^{\text{sc}}| \ll 1$  [5,6,7,14,15]. The corrections to  $f_q^{\text{sc}}$  take the following form [14]

$$\phi_q^s(t) = f_q^{\text{sc}} + h_q^s G(t) + h_q^{s(2)} \left[ \frac{t}{\tau} \right]^{2b}. \quad (2)$$

The first two terms represent the space-time factorization theorem. The spatial dependence is contained in  $f_q^{\text{sc}}$  and in the critical amplitude  $h_q^s$ , whereas the  $\beta$ -correlator  $G(t)$  carries the whole time and temperature dependence. In the idealized MCT it is given by [6,14,15]

$$G(t) = \sqrt{|\varepsilon|} g(t/t_\varepsilon) \quad \text{with} \quad t_\varepsilon = \frac{t_0}{|\varepsilon|^{1/2a}}, \quad \varepsilon = C \left[ \frac{T_c - T}{T_c} \right], \quad (3)$$

where  $t_0$  is a matching time to the microscopic transient,  $t_\varepsilon$  is the  $\beta$ -time scale,  $\varepsilon$  is the separation parameter ( $C = \text{constant}$ ), and  $g(\hat{t})$  is the temperature independent  $\beta$  master function. Its shape is determined by the exponent parameter  $\lambda$ , which in turn fixes the critical exponent  $a$  and the von-Schweidler exponent  $b$  via  $\lambda = \Gamma(1 - a)^2 / \Gamma(1 - 2a) = \Gamma(1 + b)^2 / \Gamma(1 + 2b)$ .

The third term of Eq. (2) is a leading-order correction (of order  $|\varepsilon|$ ) to  $h_q^s G(t)$  (which is of order  $|\varepsilon|^{1/2}$ ) [14,15]. It extends the description of the decay from  $f_q^{\text{sc}}$  to longer times (i.e., for  $t_\varepsilon \ll t \ll \tau$  it is a correction to the von-Schweidler law  $t^b$ ), and depends on temperature by the  $\alpha$ -time scale  $\tau$

$$\tau = t_\varepsilon \left[ \frac{t_\varepsilon}{t_0} \right]^{a/b} = \frac{t_0}{|\varepsilon|^\gamma} \quad \text{for} \quad T \geq T_c \quad (4)$$

with  $\gamma = 1/(2a) + 1/(2b)$ .

When applying these formulas to the simulation data we proceeded in two steps. First, we tried to fix the exponent parameter by working with the factorization theorem only. To this end, we calculated the  $\beta$ -scaling function for a specific value of  $\lambda$  numerically. The

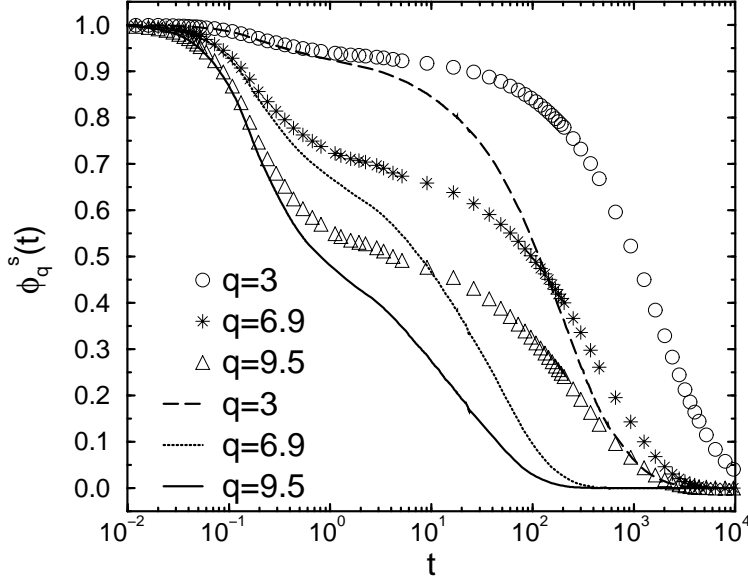


FIG. 2. Incoherent intermediate scattering functions versus time at  $T = 0.47$  (symbols) and at  $T = 0.52$  (lines). Three  $q$ -values are shown:  $q = 3$  ( $\approx$  size of the chain),  $q = 6.9$  [ $\approx$  maximum of  $S(q)$ ], and  $q = 9.5$  [ $\approx$  first minimum of  $S(q)$ ].

result was inserted in Eq. (2), and the remaining parameter,  $f_q^{\text{sc}}$ ,  $t_\varepsilon$ , and the total prefactor of  $g(\hat{t})$ ,  $\tilde{h}_q^s(T) = h_q^s |\varepsilon|^{1/2}$ , were adjusted at a given temperature and  $q$ -value. This procedure was repeated for different  $\lambda$ - and  $q$ -values (mainly  $q = 6.9, 9.5$ ), and at several temperatures (mainly  $T = 0.48, 0.52$ ) to explore which range of  $\lambda$ -values yielded fits of comparable quality. The best-fit result was:

$$\lambda = 0.635 \pm 0.025, \quad a = 0.352 \pm 0.010, \quad b = 0.75 \pm 0.04, \quad \gamma = 2.09 \pm 0.07. \quad (5)$$

In addition, this first step also helps to find the upper bound of the temperature interval, where the asymptotic formulas of MCT can be applied. For the model studied this is  $T \approx 0.52$ . Therefore, the second step was restricted to  $T \leq 0.52$ . In this step, we fixed  $\lambda = 0.635$  and optimized the remaining parameters,  $f_q^{\text{sc}}$ ,  $t_\varepsilon$ ,  $\tilde{h}_q^s$ , and  $\tilde{h}_q^{s(2)}(T) = h_q^{s(2)} \tau^{-2b}$ . This procedure was done for  $T = 0.47, 0.48, 0.49, 0.5, 0.52$ , and at about 20 different  $q$ -values, ranging from  $q = 1$  to  $q = 19$ , for each temperature.

The simulation results for  $T = 0.47$  and  $T = 0.52$  are compared in Fig. 2. The figure shows the incoherent intermediate scattering function over six decades in time<sup>2</sup> for three different wave vectors. The smallest  $q$ -value ( $q = 3$ ) probes the length scale of a chain, whereas  $q = 6.9, 9.5$  approximately correspond to the maximum and the first minimum of

---

<sup>2</sup>Time is measured in units of the MD time step, which is  $dt = 0.002$  [28]. Six decades in time therefore correspond to  $5 \times 10^6$  MD steps.

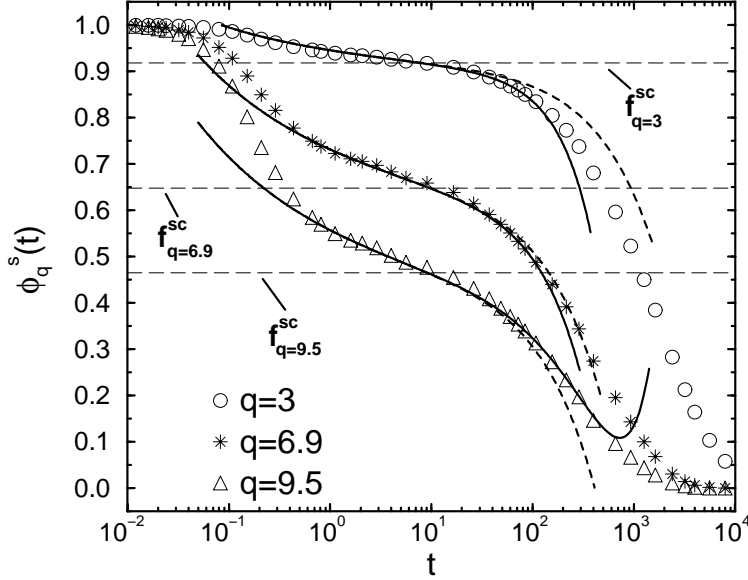


FIG. 3. Incoherent intermediate scattering function versus time at  $T = 0.47$ . Three  $q$ -values are shown:  $q = 3$  ( $\approx$  size of the chain),  $q = 6.9$  [ $\approx$  maximum of  $S(q)$ ], and  $q = 9.5$  [ $\approx$  first minimum of  $S(q)$ ]. The dashed lines are the MCT-fit results, using only the factorization theorem, whereas the solid lines also include the corrections to the von-Schweidler law. The dashed horizontal lines indicate the fit values for  $f_q^{\text{sc}}$  at the respective momentum transfers.

the structure factor  $S(q)$  (see Fig. 1). At a given  $q$ -value the simulation data almost coincide for both temperatures if  $t \leq 10^{-1}$ . This short-time regime corresponds to the ballistic motion of a monomer, which only shows a weak  $\sqrt{T}$  temperature dependence. Contrary to that, the curves strongly separate from one another with increasing time. At  $T = 0.47$ ,  $\phi_q^s(t)$  reaches zero about a decade later than at  $T = 0.52$ . To achieve a similar growth of the structural relaxation time when cooling from higher temperature to  $T = 0.52$ , one has to take  $T \approx 0.7$ , a temperature that is 35% larger than  $T = 0.52$ . Compared to this difference, the 10% disparity between  $T = 0.47$  and  $T = 0.52$  is indicative of the approach to  $T_c$ , where the asymptotic formulas, Eqs. (2)–(4), should hold.

Figures 3 and 4 show comparisons between the simulation data and Eq. (2) for  $T = 0.47$  and  $T = 0.52$ , respectively. For both temperatures the description of the data by the theory starts at about the same time,  $t \approx 0.6$ , (except at  $T = 0.52$  and  $q = 3$ , where the fits extends to  $t \leq 10^{-1}$ ). This suggests that the scale  $t_0$ , which MCT introduces as a matching time of Eq. (2) to the transient microscopics close to  $T_c$  (i.e.,  $t_0 \approx t_0(T_c) = \text{constant}$ ), is only weakly – if at all – temperature dependent for our polymer model. The same conclusion could have also been drawn from Fig. 2 because the scattering functions, calculated at different temperatures, coincide for small times (i.e., for  $t < 0.3$ ). Whereas the asymptotic result,  $t_0 \approx \text{constant}$ , appears to hold quite generally in experiments and simulations of nonpolymeric systems [2], a pronounced temperature dependence was found in a Monte

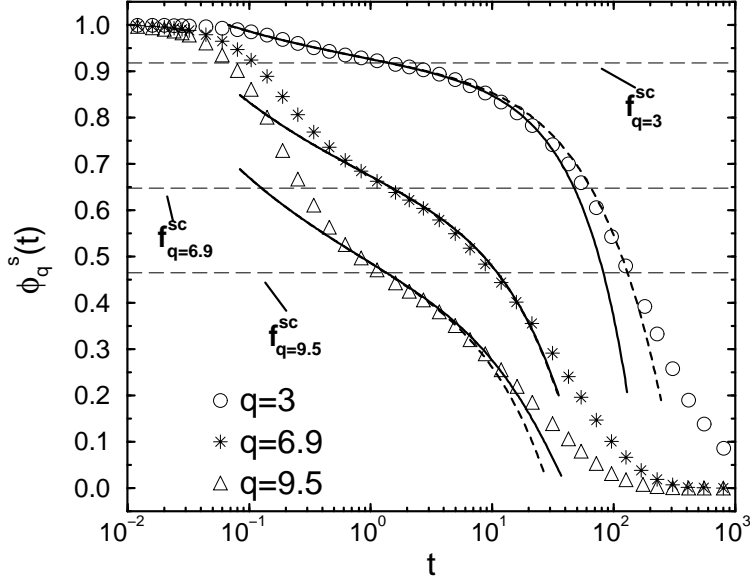


FIG. 4. Incoherent intermediate scattering function versus time at  $T = 0.52$ . Three  $q$ -values are shown:  $q = 3$  ( $\approx$  size of the chain),  $q = 6.9$  [ $\approx$  maximum of  $S(q)$ ], and  $q = 9.5$  [ $\approx$  first minimum of  $S(q)$ ]. The dashed lines are the MCT-fit results, using only the factorization theorem, whereas the solid lines also include the corrections to the von-Schweidler law. The dashed horizontal lines indicate the fit values for  $f_q^{\text{sc}}$  at the respective wave-vectors.

Carlo simulation of the bond-fluctuation model [25]. Compared to the present study, this seems to be a model-specific rather than a typical feature of glass forming polymers, contrary to the conjecture of Ref. [25].

For  $t > 0.6$ , the idealized theory describes the decay of the correlators over about 1.5 decades in time at  $T = 0.52$  and over more than 2 decades at  $T = 0.47$ . Therefore the  $\beta$ -window expands considerably in this narrow temperature interval. The extension of the window can also be inferred from the shift of the time  $\tau_{\text{co}}$ , where  $f_q^{\text{sc}}$  crosses the simulation data. For all  $q$ -values it increases from about 1.4 at  $T = 0.52$  to about 10 at  $T = 0.47$ . The independence of  $\tau_{\text{co}}$  on  $q$  is an evidence of the factorization theorem which implies  $\phi_q^s(\tau_{\text{co}}) = f_q^{\text{sc}}$  for all  $q$ , if  $G(\tau_{\text{co}}) = 0$ . As  $T \rightarrow T_c^+$ , one expects  $G(t) = 0$  to occur close to the  $\beta$ -relaxation time so that  $\tau_{\text{co}} \propto t_\epsilon$  [15]. For  $T > T_c$ ,  $t_\epsilon$  marks the crossover of the critical to the von-Schweidler dynamics, where corrections are not dominant yet. This can be seen in Figs. 3 and 4. The idealized fits with and without corrections coincide on the scale  $\tau_{\text{co}}$ , but deviate at later times. Depending on  $q$ , corrections to the von-Schweidler law extend the fits by about 0.25 decades at  $T = 0.52$  and by about 0.5 decades at  $T = 0.47$ . For  $q = 3$ , they are negative, but positive for  $q = 9.5$ . The change of sign occurs approximately around  $q = 6.9$ . This behavior qualitatively agrees with theoretical calculations for hard spheres [14] and recent simulations for linear molecules [30].

Despite this agreement, we want to mention a problem that we faced when applying



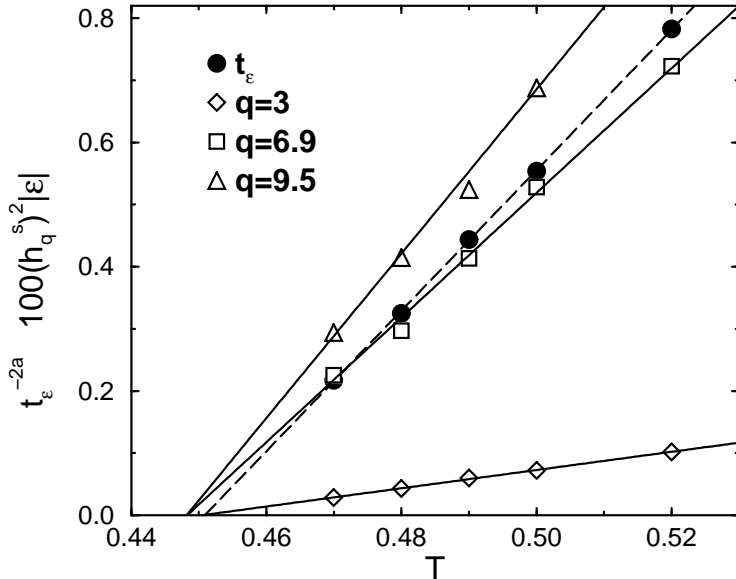


FIG. 5. Temperature dependence of the  $\beta$ -time scale,  $t_\varepsilon$ , and of the total prefactor of the  $\beta$ -scaling function,  $\tilde{h}_q^s = h_q^s |\varepsilon|^{1/2}$ . Plots of  $t_\varepsilon^{-2a}$  and of  $(\tilde{h}_q^s)^2$  versus  $T$  should extrapolate to zero at  $T_c$  [see Eq. (3)]. The fit results (dashed line for  $t_\varepsilon$  and solid lines for  $\tilde{h}_q^s$ ) can be combined to a common estimate:  $T_c = 0.450 \pm 0.005$ .

the corrections. In the analysis we treated  $\tilde{h}_q^s$  and  $\tilde{h}_q^{s(2)}$  as temperature- and  $q$ -dependent fit parameters. However, contrary to  $\tilde{h}_q^s$ , the resulting temperature dependence of  $\tilde{h}_q^{s(2)}$  turned out to be rather irregular and sometimes even opposite to the theoretical expectation, especially at low temperatures. From Eq. (2) one expects the significance of the corrections to diminish as  $T_c$  is approached, whereas Figs. 3 and 4 show that they become more important with decreasing temperature. This discrepancy could have two reasons. First,  $\tilde{h}_q^{s(2)}$  is about 2 to 3 orders of magnitude smaller than  $\tilde{h}_q^s$  (which itself is of the order  $10^{-2}$ ). Therefore it is numerically difficult to extract reliable values from the fits, especially at large  $q$ -values, where  $f_q^{sc}$  is small. Second, the idealized MCT is only supposed to work in a temperature interval which is close, but not too close to  $T_c$ . In the immediate vicinity of  $T_c$ , ergodicity restoring hopping processes [6,18] start to compete with the ergodicity breaking cage effect that is treated by the idealized MCT. Qualitatively, the main influence of the hopping processes is to accelerate the decay of the correlators at late times. Since the uncorrected idealized fits for small  $q$  lie above the simulation data, the addition of corrections to the von-Schweidler law could partly mimic the effect of hopping. This ambiguity can complicate the analysis. Presumably, it would have been better to impose the theoretical temperature dependence on  $h_q^{s(2)}$ , and to adjust only the variation with  $q$ .

Despite this proviso, the idealized analysis should yield reliable results on the  $\beta$ -time scale around  $\tau_{co}$ , where neither corrections, nor hopping processes are dominant. From the fits one can extract the  $q$ -dependences of  $f_q^{sc}$  and  $h_q^s$ , and the critical temperature. These

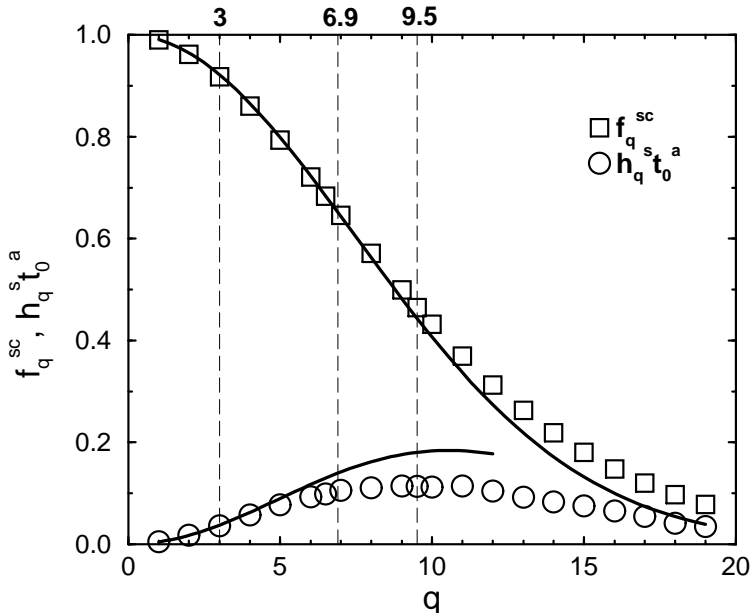


FIG. 6.  $q$ -dependence of the nonergodicity parameter  $f_q^{\text{sc}}$  and of the critical amplitude  $h_q^{\text{s}}$  (in fact,  $h_q^{\text{s}} t_0^a$  is shown). The microscopic matching time  $t_0$  cannot be separated in the fit). The solid curves are the Gaussian approximations of Eq. (6). The fit interval for  $f_q^{\text{sc}}$  was  $1 \leq q \leq 8$ . The result of this fit was used to estimate  $h_{\text{msd}}$  from the behavior of  $h_q^{\text{s}}$  at small  $q$ .

results are shown in Figs. 5 and 6. Figure 5 plots  $t_\varepsilon^{-2a}$  and  $(\tilde{h}_q^{\text{s}})^2$  versus temperature. The theoretically predicted linear behavior [see Eq. (3)] is nicely confirmed by the data. A linear regression yields  $T_c \simeq 0.451$  for  $t_\varepsilon$ . Similar estimates are obtained for  $\tilde{h}_q^{\text{s}}$ :  $T_c \simeq 0.451$  ( $q = 3$ ),  $T_c \simeq 0.448$  ( $q = 6.9$ ), and  $T_c \simeq 0.448$  ( $q = 9.5$ ). Combining these results we find  $T_c = 0.450 \pm 0.005$ , which implies  $0.04 \leq (T - T_c)/T_c \leq 0.15$  for the reduced distance to the critical point in our model. Although  $(T - T_c)/T_c = 0.04$  corresponds to the upper limit, where some of the asymptotic laws begin to be detectable in theoretical calculations for hard spheres [14,15], similar reduced distances are not unusual in practical applications of MCT (see Refs. [31,32], for instance).

Figure 6 shows the  $q$ -dependences of  $f_q^{\text{sc}}$  and  $h_q^{\text{s}}$ , together with the Gaussian approximations,

$$f_q^{\text{sc}} \approx \exp[-q^2 r_{\text{sc}}^2] \quad \text{and} \quad h_q^{\text{s}} \approx h_{\text{msd}} q^2 \exp[-q^2 r_{\text{sc}}^2], \quad (6)$$

which are supposed to hold for small  $q$  [14]. As in other experimental [33] and theoretical studies [30,34], the nonergodicity parameter of our model monotonously decreases with increasing  $q$ , whereas the critical amplitude passes through a maximum between the maximum and the first minimum of  $S(q)$ . The Gaussian approximations provide reasonable descriptions for the initial behavior of both  $f_q^{\text{sc}}$  and  $h_q^{\text{s}}$ . The description extends farther for  $f_q^{\text{sc}}$  ( $q \leq 10$ ) than for  $h_q^{\text{s}}$  ( $q \leq 4$ ), which is qualitatively comparable to the theoretical results for hard spheres [14,35]. From the fits one obtains:  $r_{\text{sc}} = 0.095 \pm 0.005$  and

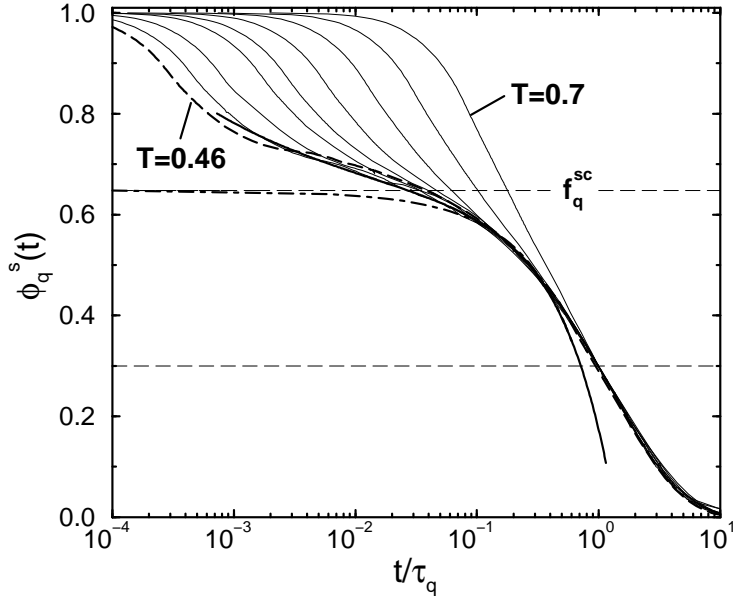


FIG. 7.  $\alpha$ -scaling plot of  $\phi_q^s(t)$  versus  $t/\tau_q$  for  $q = 6.9$ . Nine different temperatures are shown:  $T = 0.46, 0.47, 0.48, 0.49, 0.5, 0.52, 0.55, 0.6, 0.7$  (from left to right). The scaling time  $\tau_q$  was defined by  $\phi_q^s(\tau_q) = 0.3$  (lower horizontal dashed line). Note that the scaling extends to shorter rescaled times with decreasing temperature if  $T \geq 0.48$ . For  $T = 0.46$  (dashed line) this trend is violated (see text for further discussion).

$h_{\text{msd}} t_0^\alpha = 0.0045 \pm 0.0010$ . Both parameters enter the first two terms of the short-time expansion for the  $\alpha$ -process of the (monomer) mean-square displacement, which corresponds to the von-Schweidler law in reciprocal space [14]. The mean-square displacement will be briefly discussed in the next section and more extensively together with related quantities in Ref. [36].

## B. $\alpha$ -relaxation regime

The final structural decay from the nonergodicity parameter to zero is called  $\alpha$ -relaxation regime. For this regime the idealized MCT makes the following predictions [14,15,35]. First, the  $\alpha$ -process asymptotically obeys a time-temperature superposition principle,

$$\phi_q^s(t) = \tilde{\phi}_q^s(t/\tau), \quad (7)$$

i.e., all correlators, measured for one  $q$ -value at different temperatures, should collapse onto a master curve if time is rescaled by  $\tau$  [see Eq. (4)]. Second, the short-time expansion of Eq. (7) coincides with the long-time behavior of the  $\beta$ -process, i.e., with the von-Schweidler law,  $\phi_q^s(t) = f_q^{\text{sc}} - h_q^s B (t/\tau)^b$  ( $B = 0.476$  for our model). Third, the leading-order corrections to Eq. (7) extend the description beyond  $f_q^{\text{sc}}$  at short rescaled times. They are given by  $\delta \tilde{\phi}_q^s(t/\tau) = h_q^s (B_1/B) |\varepsilon| (\tau/t)^b$  (with  $B_1 = 0.185$ ), and are identical to the corrections of the

$\beta$ -correlator for  $t \gg t_\varepsilon$ . Forth, in the limit of large  $q$  the  $\alpha$  master curve is given by a Kohlrausch function [37]

$$\phi_q^s(t) = f_q^K \exp \left[ - \left( \frac{t}{\tau_q^K} \right)^{\beta_K} \right] \quad (8)$$

with  $f_q^K = f_q^{\text{sc}}$ ,  $\beta_K = b$ , and  $\tau_q^K(T) = \hat{\tau}_q^K \tau(T)$ , where  $\hat{\tau}_q^K \propto q^{-1/b}$ . On the other hand, it is found that Eq. (8) represents a good approximation for the  $\alpha$  master function even if  $q$  is small [35].

Figure 7 shows a test of these predictions for  $q = 6.9$ . A scaling time  $\tau_q$  was defined by  $\phi_q^s(\tau_q) = 0.3$ . This is legitimate because any time belonging to the  $\alpha$ -regime is expected to exhibit asymptotically the same temperature dependence, i.e.,  $\tau_q \sim \tau$ , due to time-temperature superposition. The figure shows that the time-temperature superposition property is borne out by the simulation data for  $T \leq 0.7$ . Therefore, it already starts at higher temperatures compared to the  $\beta$ -scaling. Theoretically, such a difference can be rationalized by the fact that the corrections to the  $\beta$  master function are of order  $\varepsilon^{1/2}$ , and thus larger than those of Eq. (7), which are of order  $\varepsilon$  only. At  $T = 0.7$  the  $\alpha$ -scaling is realized for about the last 40% of the decay. With decreasing temperature it extends to smaller rescaled times in such a way that it progressively adjusts to the von-Schweidler law, and deviations at shorter times are quantitatively described by the  $\beta$ -correlator.

This qualitative trend persists as long as  $T \geq 0.47$ . However, for  $T = 0.46$  the rescaled correlator moves away from the von-Schweidler asymptote instead of approaching it further. This is in contrast to the theoretical expectation. Although we could not propagate the chain over several times the radius of gyration, we believe that the melt is equilibrated over the distances probed by  $q = 6.9$  so that the deviation is presumably not a residual nonequilibrium effect. A possible explanation is that the melt at  $T = 0.46$  ( $(T - T_c)/T_c = 0.0\bar{2}$ ) is already so close to  $T_c$  that the influence of ergodicity restoring processes starts to be felt. These processes change the shape of the correlator in the von-Schweidler regime and prevent the strong increase of the  $\alpha$ -relaxation time according to Eq. (4) from continuing [18]. It is therefore possible that a correlator falls above the idealized  $\alpha$  master curve when trying to rescale it by a relaxation time which is too small. However, a comparable overshoot was not observed in a recent MD-simulation of diatomic molecules [30], although the temperature dependence of the relaxation times deviated markedly from the idealized prediction at the lowest temperatures studied. Nevertheless, the low temperature curves start crowding in the plateau regime and no longer expand along the von-Schweidler asymptote for shorter rescaled times. Therefore, it is conceivable that an overshoot could also occur in this model at still lower temperatures.

Figure 8 shows that the relaxation time at  $T = 0.46$  is indeed smaller than expected from the mode-coupling fit. The figure depicts a plot of  $\tau_q^{-1/\gamma}$  and  $D^{1/\gamma}$  ( $D$ : diffusion coefficient of a chain) versus  $T$ , using the best estimate for  $\gamma$  from the  $\beta$ -analysis ( $\gamma = 2.09$ ). In the temperature interval, in which the idealized analysis was possible ( $0.47 \leq T \leq 0.52$ ; at  $T = 0.46$  the  $\beta$ -analysis with the parameters quoted above did not yield acceptable results), the simulation results lie on straight lines, as predicted by MCT. However, for  $T = 0.46$ , the relaxation times are too small (no reliable estimate of the diffusion coefficient could be obtained after  $5 \times 10^7$  MD-steps). The same observations were also made in Ref. [30] for comparable reduced distances to the critical point. Therefore the interval  $0.47 \leq T \leq 0.52$

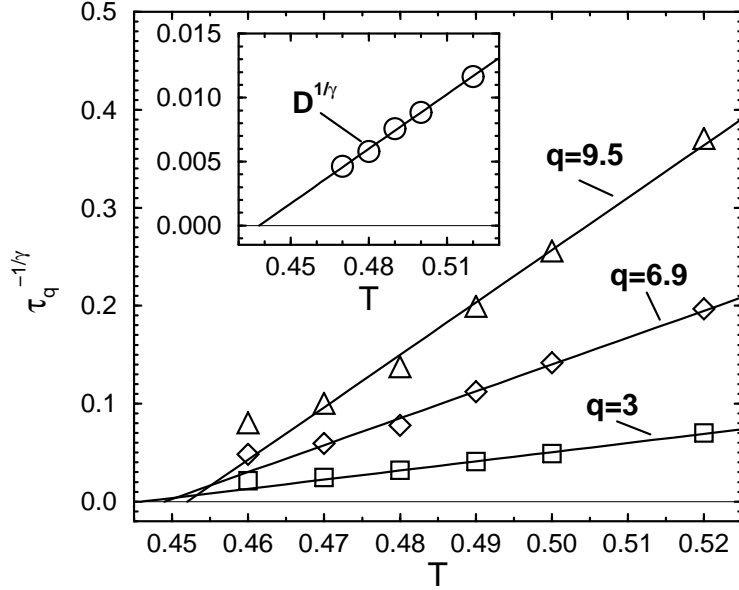


FIG. 8. Plot of  $\tau_q^{-1/\gamma}$  versus temperature for  $q = 3$  ( $\approx$  size of a chain),  $q = 6.9$  [ $\approx$  maximum of  $S(q)$ ], and  $q = 9.5$  [ $\approx$  first minimum of  $S(q)$ ]. The exponent  $\gamma$  was taken from the  $\beta$ -analysis ( $\gamma = 2.09$ ). The straight lines are fit results for the interval  $0.47 \leq T \leq 0.52$ . The intersections of the fits with the zero-line are estimates for  $T_c$ :  $T_c = 0.446$  ( $q = 3$ ),  $T_c = 0.449$  ( $q = 6.9$ ),  $T_c = 0.452$  ( $q = 3$ ). The inset shows the same plot for the diffusion constant. Here the fit result for the critical temperature is significantly smaller, i.e.,  $T_c = 0.438$ .

was used to obtain further estimates for  $T_c$ . For  $\tau_q$  this yields  $T_c \approx 0.446$  for  $q = 3$ ,  $T_c \approx 0.449$  for  $q = 6.9$ ,  $T_c \approx 0.452$  for  $q = 9.5$ , and for  $D$ ,  $T_c \approx 0.438$ . Whereas the variation of  $T_c$  for  $\tau_q$ , albeit decreasing systematically with decreasing  $q$ , is compatible, within the error bars, with  $T_c = 0.450$  from the  $\beta$ -analysis, the result from  $D$  is too small. Barring the problem that the diffusion coefficient is hard to determine accurately at low temperatures (i.e., for  $T \leq 0.47$ ), the high temperature behavior (i.e.,  $0.48 \leq T \leq 0.52$ ) suggests that the disparity in the  $T_c$ -estimates is significant. Such a finding is not uncommon. Similar observations were made in MD-simulations of a water model [38] and of a binary Lennard-Jones mixture [32]. Whereas the difference in  $T_c$  in the water simulation was small and could be attributed to numerical uncertainties, a much larger reduction was found for the binary mixture. On the other hand, an unconstrained fit yielded a critical temperature which was compatible with the estimates from coherent and incoherent scattering, but  $\gamma$  was in turn significantly smaller than that from the  $\beta$ -analysis. The same result was also obtained in MD-simulations of diatomic molecules [30,39] and for our model [29].

In experiments and simulations it is generally found that the Kohlrausch function represents a very good fit formula for the major part of the  $\alpha$ -relaxation. Only at early times deviations (can) become visible. Mode-coupling theory interpretes these deviations as a signature of the von-Schweidler law, since it concatenates the  $\beta$ - with the  $\alpha$ -process, and

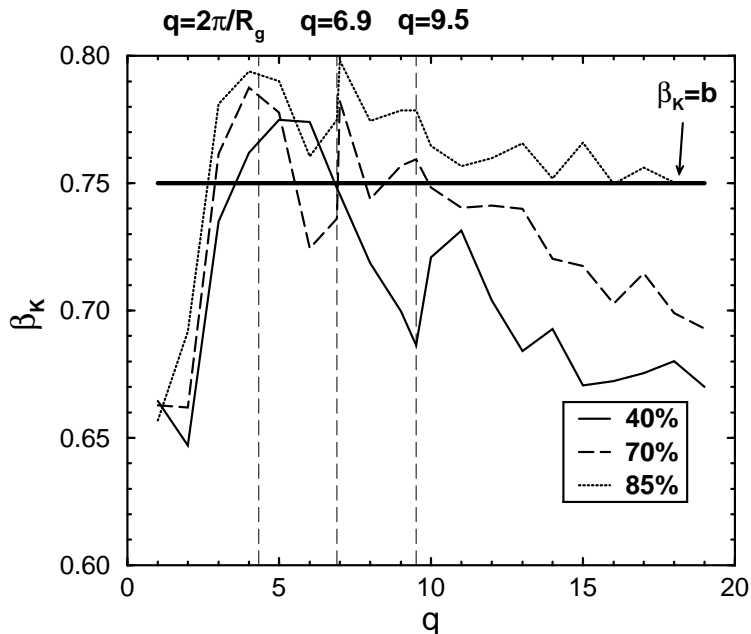


FIG. 9. Kohlrausch stretching exponent  $\beta_K$  [see Eq. (8)] as a function of  $q$  for three different choices of the fit interval  $0.02 \leq \phi_q^s(t)/f_q^{\text{sc}} \leq X$  for  $X = 0.4, 0.7$  and  $0.85$ . The thick horizontal line indicates the von-Schweidler exponent  $b = 0.75$ . In addition, three different  $q$ -values are highlighted by vertical dashed lines:  $q = 2\pi/R_g \approx 4.35$  ( $R_g =$  radius of gyration),  $q = 6.9$  [ $\approx$  maximum of  $S(q)$ ], and  $q = 9.5$  [ $\approx$  first minimum of  $S(q)$ ].

$\beta_q \neq b$  in general [35]. Therefore, when applying the Kohlrausch function, the problem arises that the late  $\beta$ -process interferes with the fit [40], and additionally, that the fit parameters sensitively depend on the size of the fit interval (for a discussion of this problem see Refs. [41,42], for instance). To lessen this problem two procedures are often used. On the one hand, one can fit the late-time decay of the  $\alpha$  master function by taking into account that the short-time bound of the fit interval should not overlap too much with the von-Schweidler regime. This procedure has been used in Refs. [30,32], for instance. On the other hand, one can work with so-called  $\alpha$ - $\beta$ -fits, in which Eq. (2) (without corrections) and Eq. (7) are superimposed. Except for hard-sphere colloidal systems, where it is possible to calculate the master function numerically [35,43], Eq. (7) is usually replaced by Eq. (8). The superposition requires  $f_q^K = f_q^{\text{sc}}$ , and the von-Schweidler law to be subtracted from the  $\beta$ -correlator because it is already approximated by the Kohlrausch function [44,45] (for an alternative procedure see [31]).

A variant of the latter approach was applied in this simulation. We only worked with the Kohlrausch function, but fixed the amplitude by  $f_q^K = f_q^{\text{sc}}$ . Then we tried to optimize the stretching exponent  $\beta_K$  (the time scale is already given by  $\phi_q^s(\tau_q^K) = f_q^{\text{sc}} e^{-1}$ ). The results are still very sensitive to the choice of the fit interval. An example is given in Fig. 9. It shows the  $q$ -dependence of the stretching exponent  $\beta_K$ . The percentages specify the portion of the decay from  $f_q^{\text{sc}}$  to (about) 0, which is included in the fit (i.e., “40%” means the range

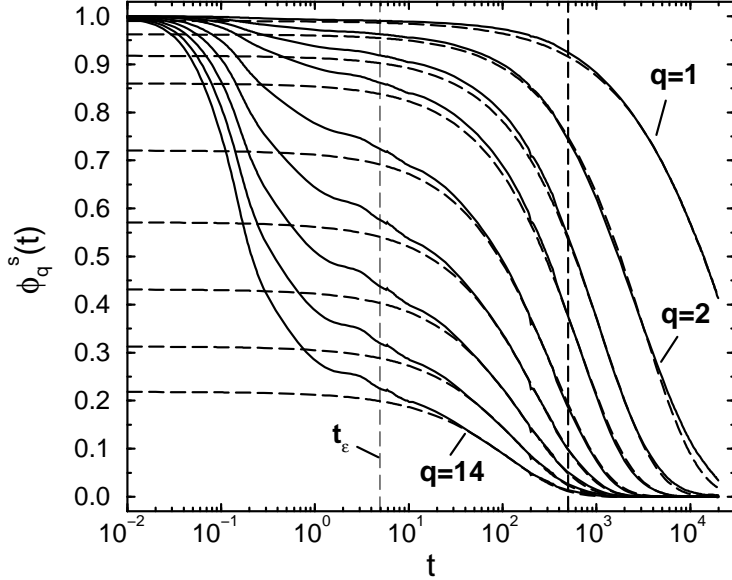


FIG. 10.  $\phi_q^s(t)$  and Kohlrausch functions at  $T = 0.48$ . Solid lines are the simulation data for nine different  $q$ -values:  $q = 1, 2, 3, 4, 6, 8, 10, 12, 14$  (from right to left). For  $q \geq 2$ , the Kohlrausch parameters are given by:  $f_q^K = f_q^{\text{sc}}$ ,  $\beta_K = b = 0.75$ , and  $\tau_q^K$  from  $\phi_q^s(\tau_q^K) = f_q^{\text{sc}} e^{-1}$ . These choices provide a good description of the  $\alpha$ -decay, as long as  $q > 2$ . For  $q \leq 2$ , deviations gradually develop. The stretching becomes more pronounced, leading to the following parameters at  $q = 1$ :  $f_q^K = f_q^{\text{sc}}$ ,  $\beta_K = 0.656$ , and  $\tau_q^K = 24595$ . In addition, two vertical lines are shown. The thin dashed line is  $t_\epsilon(T = 0.48) = 4.933$ , whereas the thick dashed line indicates the lower time value ( $t = 500$ ), above which the monomer mean-square displacement exhibits a  $t^{0.65}$ -behavior (see Fig. 11).

$0.02 \leq \phi_q^s(t)/f_q^{\text{sc}} \leq 0.4$ ). At large  $q$  the nonergodicity parameter is so small that statistical noise of the data considerably influences the results. The  $\beta_K$ -values for the various fit intervals then strongly splay out, leading to a difference of about 15% at  $q = 19$ . With decreasing  $q$  the curves approach one another and fluctuate around  $\beta_K \approx b = 0.75$ , except for the smallest  $q$ -values,  $q = 1, 2$ , where  $\beta_K$  lies between 0.65 and 0.7.

This behavior suggests that it should be possible to find a fit interval for  $q > 2$ , where the Kohlrausch function with  $f_q^K = f_q^{\text{sc}}$  and  $\beta_K = b$  provides a good description of the  $\alpha$ -process. Figure 10 shows a comparison between  $\phi_q^s(t)$  and such Kohlrausch functions for a selection of  $q$ -values, ranging from  $q = 1$  to  $q = 14$ , at  $T = 0.48$ . One can clearly see that the expectation  $\beta_K = b$  is well borne out if  $q \geq 3$ , but that smaller stretching exponents are required for  $q < 3$ .

In addition, the data exhibit a small bump at about  $t = 3$  for all wave vectors. This bump gradually develops at low temperatures ( $T < 0.52$ ), but is hard to see in the presentation of Figs. 2 or 3. A similar feature was also observed in other simulations of fragile glass formers, for instance, for orthoterphenyl [41] or for a binary Lennard-Jones mixture [34], and is much more pronounced for strong glasses, like silica [46]. Usually, the bump is attributed to a finite size effect. Due to nonlinear coupling with other wave vectors a sound wave, which

propagates through the simulation box, leaves it on one side, and immediately reenters the box on the other side because of periodic boundary conditions, could generate a disturbance at a time  $t \approx L/c$ , where  $L$  is the linear dimension of the box and  $c$  is the sound velocity. Using  $L = 10.5$ , and estimating the sound velocity as  $c \approx 7$ ,<sup>3</sup> we find  $t \approx 1.5$ , which is close to the position of the bump.

Two comments with respect to the Kohlrausch fits have to be made. First, the equality  $\beta_K = b$  starts to work at  $q$ -values which are about a factor of 2 smaller than the maximum position of  $S(q)$ . Such a behavior has neither been observed in experiments [44,45] nor in simulations [32] of nonpolymeric glass formers. Theoretically, one expects  $\beta_K = b$  to become valid if  $q \rightarrow \infty$ , and numerical calculations for hard spheres indicate that this limit is approximately realized only for  $q$ -values which are 5–6 times larger than the maximum position of  $S(q)$  [35,37]. Therefore the present finding seems to be a special property of the model under consideration, although neutron-scattering experiments for polybutadiene [16,47] and other polyolefines [48,49] also suggest  $\beta_K = \text{const}$  (and perhaps  $\approx b$  for polybutadiene [16]) for  $q$ -values that lie around the maximum of  $S(q)$  (typically,  $2\pi/R_g \ll 0.2 \leq q \leq 5 \text{ \AA}^{-1}$ ).

The second comment concerns the drop of  $\beta_K$  for small  $q$ . Usually, one expects  $\beta_K$  to increase monotonously to 1 as  $q \rightarrow 0$  because the system becomes freely diffusive on this length scale. This behavior is well borne out in theoretical calculations for hard spheres [35] and simulations of simple liquids [34]. We believe that the difference observed here is related to the polymeric character of our model because  $q \leq 2$  probes the length scale of a chain. For these  $q$ -values the Gaussian approximation,

$$\phi_q^s(t) = \exp \left[ -\frac{1}{6} q^2 g_0(t) \right], \quad (9)$$

represents a (very) good description of the data (see Fig. 11) so that one can interpret the decay of  $\phi_q^s(t)$  in terms of the monomer mean-square displacement<sup>4</sup>  $g_0(t)$ . At early times ( $t \leq 0.03$ ) the mean-square displacement is purely ballistic, i.e.,  $g_0(t) = 3Tt^2 = 1.44t^2$  ( $T = 0.48$ ), before it crosses over to a plateau regime at about  $t \approx 0.3$ . At this time, Eq. (9) also ceases to be a good approximation for  $\phi_q^s(t)$ , if  $q$  is too large (i.e., for  $q \geq 5$ ). The leveling-off of  $g_0$  reflects the temporary localization of the monomers in their cages. It is the counterpart of the  $\beta$ -relaxation in real space, and can be described by [14]

$$g_0(t) \simeq 6r_{\text{sc}}^2 - 6h_{\text{msd}} \left[ \frac{t_0}{t_\varepsilon} \right]^a g(t/t_\varepsilon) - 6h_{\text{msd}} C_a \left[ \frac{t_0}{t} \right]^{2a} - 6h_{\text{msd}} B^2 C_b \left[ \frac{t_0}{t_\varepsilon} \right]^{2a} \left[ \frac{t}{t_\varepsilon} \right]^{2b}, \quad (10)$$

where  $C_a$  and  $C_b$  are constants, which result from the corrections to the critical decay and to the von-Schweidler law in the limit  $q \rightarrow 0$ , respectively. For hard spheres, one expects  $C_a < 0$  and  $C_b < 0$  [14,15]. Figure 11b includes a fit of Eq. (10) to  $g_0(t)$ . Please note that  $r_{\text{sc}}^2 = 0.009$

---

<sup>3</sup>The sound velocity is estimated from  $c = (c_p/c_V \rho \kappa_T)^{1/2}$  by taking into account  $S(q \rightarrow 0) = T \rho \kappa_T$  and the thermodynamic relation between the specific heats,  $c_p$  and  $c_V$ , and the thermal expansion coefficient.

<sup>4</sup>All monomers are included in  $g_0(t)$ , as it was the case in the calculation of  $\phi_q^s(t)$ . For a further discussion of this and other mean-square displacements see Ref. [36].



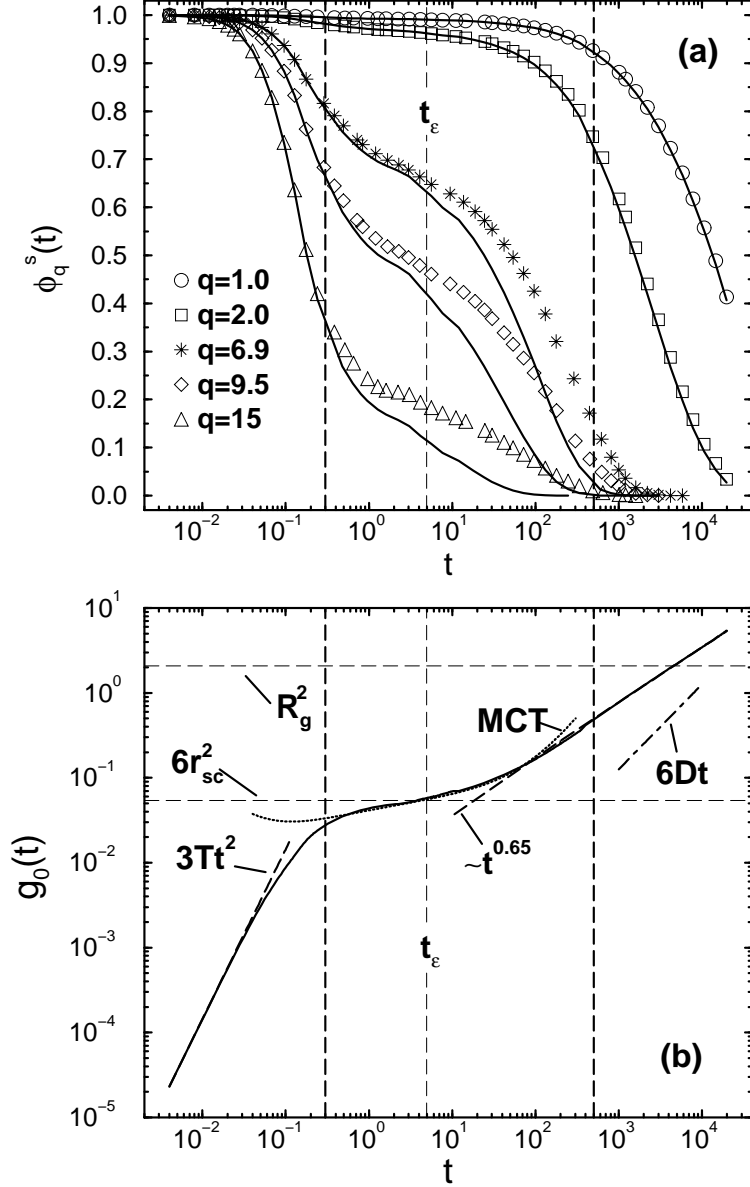


FIG. 11. Panel (a) shows a comparison between  $\phi_q^s(t)$  (symbols) and the Gaussian approximation Eq. (9) (solid lines) for five different  $q$ -values at  $T = 0.48$ . The  $q$ -values smaller than 3 probe the size of a chain (see Fig. 1). For  $q = 1$  ( $< 2\pi/R_e$ ) the agreement is quantitative. Panel (b) shows the mean-square displacement,  $g_0(t)$ , of all monomers (solid line) at  $T = 0.48$ . The initial slope is  $g_0(t) = 3Tt^2 = 1.44t^2$  (dashed line). The dotted line is a fit by Eq. (10) with  $6r_{sc}^2 = 0.054$  (dashed horizontal line). In addition, a power law,  $g_0(t) \sim t^{x_0}$  with  $x_0 = 0.65$ , is indicated by another dashed line. To determine  $x_0$ , only the simulation data larger than  $R_g^2 = 2.09$  were used. Nevertheless, the power law extends by about one decade to smaller times. The dash-dotted line shows the expected long time behavior  $g_0(t) = 6Dt$ . The diffusion coefficient was determined from the mean-square displacement of a chain, which reaches the diffusive limit earlier than  $g_0(t)$  [36]. In both panels three vertical dashed lines are shown. From left to right, the first ( $t = 0.3$ ) indicates the approximate time, when the Gaussian approximation stops working, if  $q \geq 5$ , the second is the  $\beta$ -time scale  $t_\epsilon(T = 0.48) = 4.933$ , and the last marks the onset of the  $t^{0.65}$  power law.

( $r_{\text{sc}} \simeq 0.095$  corresponds to the Lindemann criterion of melting),  $h_{\text{msd}}t_0^a = 0.0045$ ,  $t_\varepsilon = 4.933$ ,  $B = 0.476$ , and  $g(\hat{t})$  are taken from the  $\beta$ -analysis. The only adjustable parameters are  $C_a t_0^a$  and  $C_b t_0^a$ . The fit yields the reasonable values  $C_a t_0^a \approx -0.3$  and  $C_b t_0^a \approx -0.25$ . On the other hand, it is also possible to fit  $g_0(t)$  by the leading-order ansatz  $g_0(t) = 6r_{\text{sc}}^2 + At^b$ , where  $r_{\text{sc}}^2$  and  $A$  have to be adjusted [50] (see also Ref. [32] for another application to simple liquids). Although such a fit extends the description of Eq. (10) at late times by approximately one decade, it requires  $r_{\text{sc}} \approx 0.087$  and  $A \approx 3.68 \times 10^{-3}$ . These values are considerably different from those of the  $\beta$ -analysis. Therefore, the first approach should be preferred.

Equation (10) describes the simulation data from  $t \approx 0.5$  to about  $t \approx 100$ , i.e., up to the initial relaxation of a monomer out of its cage. During the  $\beta$ - and the early  $\alpha$ -relaxation a monomer hardly feels the bonds to its neighbors along the chain. The mean-square displacement is of the order  $10^{-2} - 10^{-1}$  of the monomer diameter. Therefore the monomer behaves like a particle in a simple liquid. For larger displacements chain connectivity starts to influence the monomer dynamics, and finally becomes dominant. Whereas the von-Schweidler behavior crosses over to free diffusion in simple liquids [32], a further subdiffusive regime,  $g_0(t) \sim t^{x_0}$  ( $x_0 \approx 0.65$ ), intervenes for our model if  $t \geq 500$ . Such subdiffusive displacements are well known in polymer simulations of nonentangled chains [51], and usually interpreted as a crossover between a  $t^{1/2}$ -behavior – the prediction of the Rouse model [52] for  $1 \ll g_0(t) \ll R_e^2$  – and free diffusion. A comparison of Figs. 10 and 11 shows that the subdiffusive displacement occurs in the same time regime, where the stretched exponential with  $\beta_K = 0.656$  fits  $\phi_q^s(t)$  for  $q = 1$ . Therefore, we suggest that the drop of  $\beta_K$  is a polymer specific effect, related to chain connectivity, which becomes visible if  $q$  probes the length scales between the monomer diameter ( $= 1$  in our units) and the end-to-end distance  $R_e$ . On the other hand, if  $q \ll 2\pi/R_e$ , the monomer displacement has to become diffusive, and so  $\beta_K$  should approach 1, as in simple liquids. Therefore we expect  $\beta_K$  to exhibit a minimum for our model at small  $q$ .

Finally, Fig. 12 shows the  $q$ -dependence of the  $\alpha$ -relaxation time  $\tau_q$ . Here,  $\tau_q$  was defined by  $\phi_q^s(\tau_q) = f_q^{\text{sc}}/2$  instead of by  $\tau_q^K$  because  $\tau_q^K$  is larger than the simulated times if  $q < 8$ . However, for  $q$ -values, where both times are available, we checked that they qualitatively yield the same result. In addition,  $\tau_q$  was divided by  $t_\varepsilon^{1+a/b}$  to eliminate the critical dependence on  $T_c$  [see Eq. (4)]. Asymptotically, the resulting quantity,  $\tilde{\tau}_q = \hat{\tau}_q t_0^{-a/b}$  [see Eq. (8)], should be temperature independent. The figure shows that the division does not completely remove the temperature dependence. For  $q = 1$  the relaxation times at  $T = 0.47$  and  $T = 0.52$  are about a factor of 2 different, with  $\tilde{\tau}_q(T = 0.47) < \tilde{\tau}_q(T = 0.52)$ , whereas both  $\tilde{\tau}_q$ 's first approach, and then cross one another around the first peak of the static structure factor ( $q \simeq 6.9$ ), before splaying out again. At  $q = 19$  there is again about a factor of 2 between  $T = 0.47$  and  $T = 0.52$ , but now  $\tilde{\tau}_q(T = 0.47) > \tilde{\tau}_q(T = 0.52)$ . However, the absolute values of  $\tilde{\tau}_q$  are of the order  $10^{-1}$  for  $q = 19$ , and thus 1–2 orders of magnitude smaller than  $t_\varepsilon^{1+a/b}$ , while they are comparable to  $t_\varepsilon^{1+a/b}$  at  $q = 1$ . Therefore the difference at small  $q$  seems to be more important. It could again indicate that the relaxation times on the largest length scales do not increase as rapidly as expected from idealized MCT, an observation, which we have already made for the diffusion coefficient (see Fig. 8 and Ref. [29] for further discussion of this point). On the other hand, it is not clear how significant the found deviations are at all, since the dominant temperature dependence has been taken into account by  $t_\varepsilon^{1+a/b}$ , and an additional smooth temperature dependence is expected, if  $T$  is

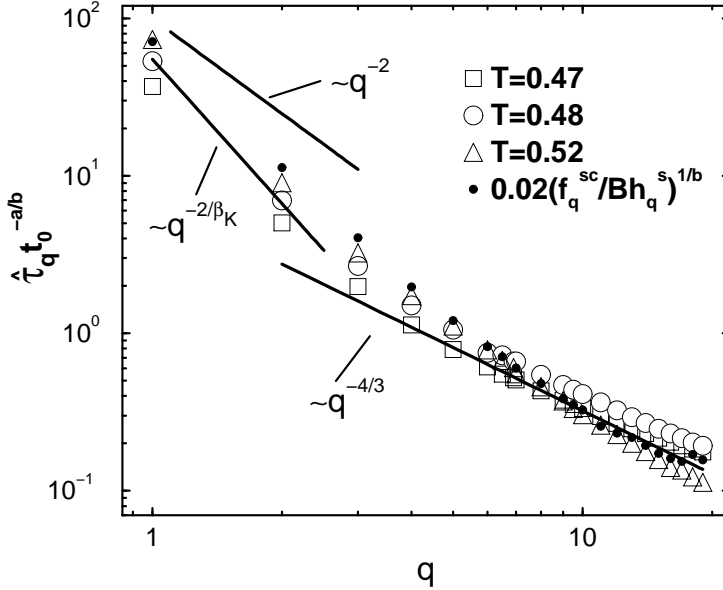


FIG. 12.  $q$ -dependence of the  $\alpha$ -relaxation time  $\tau_q$ , defined by  $\phi_q^s(\tau_q) = f_q^{sc}/2$ . The figure shows  $\hat{\tau}_q t_0^{-a/b} = \tau_q/t_\varepsilon^{1+a/b}$  [see Eq. (4)] for three different temperatures from the interval, where the  $\beta$ -analysis could be done. Thick solid lines indicate different asymptotic behavior. The initial decrease of  $\hat{\tau}_q t_0^{-a/b}$  is steeper than  $q^{-2}$ , the expected dependence for free diffusion, but compatible with  $q^{-2/\beta_K} = q^{-3.05}$  ( $\beta_K = 0.656$ ) [see Eq. (11)]. For larger  $q$ ,  $\hat{\tau}_q t_0^{-a/b}$  crosses over to the mode-coupling result, Eq. (12). The filled points show  $(f_q^{sc}/Bh_q^s)^{1/b}$ , whereas the solid line is the asymptotic limit,  $\sim q^{-1/b}$ , for  $q \rightarrow \infty$ .

not very close to  $T_c$  (see Fig. 7 of Ref. [15], for instance).

The  $q$ -dependence of the  $\alpha$ -relaxation time can be roughly divided into two regions. For  $q < 2$  Figs. 10 and 11 showed that the Gaussian approximation, Eq. (9), and the Kohlrausch function with  $\beta_K = 0.656$  describe the  $\alpha$ -relaxation of  $\phi_q^s(t)$  well. In the  $\alpha$ -regime one can therefore approximately equate Eqs. (8) and (9). Furthermore, if one assumes a power law for the  $q$ -dependence of  $\tau_q$ , one obtains

$$\tau_q \sim q^{-2/\beta_K} = q^{-3.05} \quad \text{for } q < 2. \quad (11)$$

Figure 12 shows that this estimate reasonably agrees with the initial behavior of  $\tau_q$ . Equation (11) has been suggested already some time ago in neutron-scattering experiments of glass-forming polymers [16,48], if  $q^2 g_0(t)$  is sufficiently small to warrant the Gaussian approximation (see also Ref. [47] for a critical discussion of this issue). If  $q \geq 5$ ,  $\hat{\tau}_q$  is indicative of another power-law behavior that is compatible with the mode-coupling prediction [35,37],

$$\hat{\tau}_q = \left[ \frac{f_q^{sc}}{Bh_q^s} \right]^{1/b} \xrightarrow{q \rightarrow \infty} q^{-1/b}, \quad (12)$$

which is expected to hold, if  $\beta_K = b$ . A similar observation was made in neutron-scattering experiments of orthoterphenyl [33].

## IV. CONCLUSIONS

This paper presents results of a molecular-dynamics simulations for a simple model of a glassy, nonentangled polymer melt. The discussion focuses on the monomer dynamics above  $T_c$ , as monitored by the incoherent intermediate scattering function  $\phi_q^s(t)$  and the mean-square displacement. These functions do not distinguish between bonded and nonbonded monomers so that it is *a priori* not clear how the polymeric character influences  $\phi_q^s(t)$  in the supercooled state. From the analysis the following picture emerges:

1. At very early times the motion of a monomer is purely ballistic. This corresponds to the phonon contribution in laboratory glass formers.
2. At later times, the ballistic motion slows down because the monomer feels the confinement imposed by its nearest neighbors. The monomer becomes almost localized, and the period of this localization extends over about two decades in time in the narrow temperature interval  $0.47 \leq T \leq 0.52$ . “Localization” in this context means that the mean-square displacement remains close to  $r_{sc} \approx 0.095$ , i.e., to a displacement that is about 10% of the monomer diameter. This is the regime of the  $\beta$ -relaxation, which deals with the approach towards and leaving of the plateau value  $r_{sc}$  (see Fig. 11b). In this sense,  $r_{sc}$  can be interpreted as a dynamic measure of the size of the cage. Motions on this length scale are so small that they are hardly affected by the polymeric character, i.e., by the nature of the glass former. This is presumably the reason, why mode-coupling theory, a theory developed for simple liquids, can give a reasonable explanation for the dynamics of structurally much more complicated systems in the  $\beta$ -regime.
3. Concerning the comparison with the idealized MCT in the  $\beta$ -regime, the simulation provides evidence for the space-time factorization theorem with temperature independent  $f_q^{sc}$ ,  $h_q^s$ , and  $\lambda$ , as long as  $0.47 \leq T \leq 0.52$ . In this temperature region, the  $\beta$ -relaxation time exhibits the predicted power law, yielding a critical temperature of  $T_c \simeq 0.45$ , and the  $q$ -dependences of  $f_q^{sc}$  and  $h_q^s$  are in qualitative agreement with calculations for hard spheres. For  $T < 0.47$ , deviations from the idealized behavior are observed, which can be interpreted in terms of ergodicity restoring hopping processes. We have not attempted an extended MCT-analysis because data for only one temperature below  $T = 0.47$  had been simulated. However, we can roughly estimate an upper bound of the hopping parameter  $\delta$  for our model. Using  $\delta t_0 = (t_0/t_\varepsilon)^{1+2a}$  [18],  $t_\varepsilon(T = 0.47) = 8.75$ , and assuming  $t_0 \approx 0.3$  (due to Fig. 11), we obtain  $\delta t_0 \approx 3 \times 10^{-3}$ , which would be larger than experimental values at similar distances from the critical point [31,42].
4. When the mean-square displacement becomes larger than  $r_{sc}$ , the monomer begins to leave its cage, and the temporarily frozen structure “melts” (Lindemann criterion). The initial stage of this “melting”, i.e., of the  $\alpha$ -process, can be described by the von-Schweidler law. But for larger times, polymer specific properties start dominating the dynamics. For instance, the mean-square displacement exhibits a subdiffusive behavior between the von-Schweidler law and free diffusion due to chain connectivity. The exponent of the corresponding power law is typical of the short chains studied.

It also determines the Kohlrausch stretching exponent for small wave-vectors, where the Gaussian approximation holds. Qualitatively, this difference between  $\alpha$ - and  $\beta$ -processes is expected by mode-coupling theory because the space-time factorization of the  $\beta$ -regime, which implies the same dynamics on all length scale, is no longer valid in the late  $\alpha$ -regime. However, the theory still predicts that the diffusion coefficient and the  $\alpha$ -relaxation time  $\tau_q$  should exhibit the same temperature dependence. In this respect, we find deviations between theory and simulation. The diffusion coefficient does not decrease as quickly as  $\tau_q$  at the maximum of the structure factor with decreasing temperature. Somehow the melt stays more mobile on large length scales than on local ones. On the other hand, we find evidence for the time-temperature superposition principle for the  $\alpha$ -process, if  $T \geq 0.47$ .

5. The wave-vector dependence of the  $\alpha$ -relaxation time consists of two regimes. For small  $q$ , where the Gaussian approximation holds, we find a  $q^{-2/\beta\kappa}$ -behavior, as in some neutron-scattering experiments [16,48], which crosses over to a  $q^{-1/b}$ -behavior for  $q \geq 5$ . The latter power law is a MCT-prediction for  $q$ -values much larger than the maximum of  $S(q)$ . Why this asymptotic behavior can already be observed for rather small  $q$  in the present model, is not clear.

In summary, the dynamics of our model in the supercooled state can be understood as an interplay of mode-coupling and polymer specific effects. The ‘‘caging’’ of a monomer by its neighbors leads to a temporary trapping of the monomers and to a concomittant slowing down of the structural relaxation, as in simple liquids. This cage effect is dominant, as long as the monomer displacement is small (i.e., much smaller than the diameter of a monomer). The polymeric character of the model only determines the nonuniversal parameters of MCT. However, if a monomer gradually leaves its cage, chain connectivity becomes more and more influential. For the present model of short nonentangled chains, it leads to a subdiffusive Rouse-like displacement. The subdiffusive behavior interferes with the late- $\beta$ /early- $\alpha$  dynamics and limits the von-Schweidler regime to a range, which is much smaller than in simple Lennard-Jones liquids, before free diffusion sets in.

#### ACKNOWLEDGEMENT

We are indebted to Prof. K. Binder and Drs. W. Kob, A. Latz and B. Dünweg for many helpful discussions, and to Prof. K. Binder and Dr. W. Kob for a critical reading of the manuscript. We also like to thank Dr. M. Fuchs for valuable comments which influenced the final presentation of the data very much. In the course of this work, we have profited from generous grants of simulation time by the computer center at the university of Mainz and the HLRZ Jülich, which are gratefully acknowledged, as well as financial support by the Deutsche Forschungsgemeinschaft under SFB262/D2.

- [1] Proceedings of the 2nd International Discussion Meeting on Relaxations in Complex Systems, edited by K. L. Ngai, E. Riande and G. B. Wright [*J. Non-Cryst. Solids* **172-174**, (1994)].
- [2] *Transport Theory and Statistical Physics*, edited by S. Yip and P. Nelson (Marcel Dekker, New York, 1995), Vol. 24, No. 6–8.
- [3] W. Kob, in *Supercooled Liquids: Advances and Novel Applications*, edited by J. T. Fourkas, D. Kivelson, U. Mohanty and K. A. Nelson (ACS Symposium Series 676, Washington, 1997), pp. 28–44.
- [4] W. Kob, in *Annual Reviews of Computational Physics*, edited by D. Stauffer (World Scientific, Singapore, 1995), Vol. 3, pp. 1–43.
- [5] W. Götze and L. Sjögren, *Rep. Prog. Phys.* **55**, 241 (1992).
- [6] W. Götze, in *Liquids, Freezing and the Glass Transition*, edited by J. P. Hansen, D. Levesque and J. Zinn-Justin (North-Holland, Amsterdam, 1990), Part 1, pp. 287–503.
- [7] W. Götze and L. Sjögren, in *Transport Theory and Statistical Physics*, edited by S. Yip and P. Nelson (Marcel Dekker, New York, 1995), Vol. 24, No. 6–8, pp. 801–853.
- [8] W. Götze and L. Sjögren, *Phys. Rev. A* **43**, 5442 (1991).
- [9] J.-L. Barrat and A. Latz, *J. Phys.: Condens. Matter* **2**, 4289 (1990).
- [10] M. Nauroth and W. Kob, *Phys. Rev. E* **55**, 657 (1997).
- [11] X. C. Zeng, D. Kivelson and G. Tarjus, *Phys. Rev. E* **50**, 1711 (1994); P. K. Dixon, N. Menon and S. R. Nagel, *ibid.* **50**, 1717 (1994); H. Z. Cummins and G. Li, *ibid.* **50**, 1720 (1994).
- [12] T. Franosch, W. Götze, M. R. Mayr and A. P. Singh, *Phys. Rev. E* **55**, 3183 (1997).
- [13] T. Scheidsteger and R. Schilling, *Phys. Rev. E* **56**, 2932 (1997).
- [14] M. Fuchs, W. Götze and M. R. Mayr, *Phys. Rev. E*, in press.
- [15] T. Franosch, M. Fuchs, W. Götze, M. R. Mayr and A. P. Singh, *Phys. Rev. E* **55**, 7153 (1997).
- [16] R. Zorn, D. Richter, B. Frick and B. Farago, *Physica A* **201**, 52 (1993).
- [17] A. Hofmann, F. Kremer and E. W. Fischer, *Physica A* **201**, 106 (1993).
- [18] M. Fuchs, W. Götze, W. Hildebrand and A. Latz, *J. Phys.: Condens. Matter* **4**, 7709 (1992).
- [19] H. Eliasson, B.-E. Mellander and L. Sjögren, *Mode-Coupling Analysis of Amorphous PET*, preprint.
- [20] L. Sjögren, *J. Phys.: Condens. Matter* **3**, 5023 (1991).
- [21] I. C. Halalay, *J. Phys.: Condens. Matter* **8**, 6157 (1996).
- [22] K. Binder, J. Baschnagel, S. Böhmer and W. Paul, *Phil. Mag. B* **77**, 591 (1998).
- [23] J. Baschnagel, *J. Phys.: Condens. Matter* **8**, 9599 (1996).
- [24] W. Paul and J. Baschnagel, in *Monte Carlo and Molecular Dynamics Simulations in Polymer Science*, edited by K. Binder (Oxford University Press, New York, 1995), pp. 307–355.
- [25] J. Baschnagel and M. Fuchs *J. Phys.: Condens. Matter* **7**, 6761 (1995).
- [26] W. Kob and J.-L. Barrat, *Phys. Rev. Lett.* **78**, 4581 (1997).
- [27] J.-P. Bouchaud, L. F. Cugliandolo, J. Kurchan and M. Mézard, in *Spin Glasses and Random Fields*, edited by A. Young (World Scientific, Singapore, 1998), pp. 161–223.
- [28] C. Bennemann, W. Paul, K. Binder and B. Dünweg, *Phys. Rev. E* **57**, 843 (1997).
- [29] C. Bennemann, W. Paul, J. Baschnagel and K. Binder, *Investigating the influence of different thermodynamic paths on the structural relaxation in a glass forming polymer melt*, submitted to *J. Phys.: Condens. Matter*.
- [30] S. Kämmerer, W. Kob and R. Schilling, *Phys. Rev. E* **58**, 2131 (1998).
- [31] H. Z. Cummins, G. Li, W. Du, Y. H. Hwang and G. Q. Shen, *Prog. Theo. Phys. Suppl.* **126**, 21 (1997).

- [32] W. Kob and H. C. Andersen, *Phys. Rev. E* **51**, 4626 (1995).
- [33] W. Petry, E. Bartsch, F. Fujara, M. Kiebel, H. Sillescu and B. Farago, *Z. Phys. B* **83**, 175 (1991).
- [34] W. Kob and H. C. Andersen, *Phys. Rev. E* **52**, 4134 (1995).
- [35] M. Fuchs, I. Hofacker and A. Latz, *Phys. Rev. A* **45**, 898 (1992).
- [36] C. Bennemann, J. Baschnagel, W. Paul and K. Binder, *Molecular-Dynamics Simulation of a Glassy Polymer Melt: Rouse Modes and Mean-Square Displacements*, in preparation.
- [37] M. Fuchs, *J. Non-Cryst. Solids* **172–174**, 241 (1994).
- [38] F. Sciortino, L. Fabian, S.-H. Chen and P. Tartaglia, *Phys. Rev. E* **56**, 5397 (1997).
- [39] S. Kämmerer, W. Kob and R. Schilling, *Phys. Rev. E* **56**, 5450 (1998).
- [40] M. Fuchs, W. Götze, W. Hildebrand and A. Latz, *Z. Phys. B* **87**, 43 (1992).
- [41] L. J. Lewis and G. Wahnström, *Phys. Rev. E* **50**, 3865 (1994).
- [42] H. Z. Cummins, W. M. Du, M. Fuchs, W. Götze, S. Hildebrand, A. Latz, G. Li and N. J. Tao, *Phys. Rev. E* **47**, 4223 (1993).
- [43] W. van Meegen and S. M. Underwood, *Phys. Rev. E* **49**, 4206 (1994).
- [44] M. Fuchs, H. Z. Cummins, W. M. Du, W. Götze, A. Latz, G. Li and N. J. Tao, *Phil. Mag. B* **71**, 771 (1995).
- [45] E. Bartsch, *J. Non-Cryst. Solids* **193**, 384 (1995).
- [46] J. Horbach, W. Kob, K. Binder and C. A. Angell, *Phys. Rev. E* **54**, R5897 (1996).
- [47] R. Zorn, *Phys. Rev. B* **55**, 6249 (1997).
- [48] J. Colmenero, *Macromol. Symp.* **94**, 105 (1995).
- [49] J. Colmenero, *Physica A* **201**, 38 (1993).
- [50] K. Binder, C. Bennemann, J. Baschnagel and W. Paul, *Anomalous diffusion of polymers in supercooled melts near the glass transition*, to be published by Springer Verlag, Berlin.
- [51] K. Binder and W. Paul, *J. Polymer Sci. Part B: Polymer Physics* **35**, 1 (1997).
- [52] M. Doi and S. F. Edwards, *The Theory of Polymer Dynamics* (Clarendon Press, Oxford, 1986).